Optics Communications 99 (1993) 350–354
North-Holland

OPTICS
COMMUNICATIONS

Scaling of diode-array-pumped solid-state lasers via self-imaging

A.Yu. Okulov
P.N. Lebedev Physical Institute of the Academy of Sciences of Russia, Moscow, Russian Federation

Received 11 February 1993

A new geometry of a resonator for diode-array pumped solid-state laser is analysed. A numerical modelling showed that a longitudinally pumped thin solid-state slice with transversely periodic distribution of inversion could select spatially periodic (Talbot) modes, with a diffraction limited far field, the Fresnel number being equal to the square of periods of inversion. The influence of spatial inhomogeneity of the gain, gain saturation, finite aperture and roughness of the mirrors is considered. It is found that a fundamental gaussian mode picture, typical for the single diode pumping, is gradually transformed into a transversely periodic mode along with the increase of the number of elements in the diode array, if the resonator length is half or quart of the Talbot one. It is shown that perfect in-phase lasing from the whole aperture is possible only for a limited number of elements because of the small phase distortions induced by the roughness of the mirrors and the thermal lenses inside the active slice.

1. Introduction

It is well known that diode-pumped solid-state lasers exhibit a high efficiency at low and moderate powers being pumped by a single laser diode along the optical axis of the resonator. The further increasing of the power is being achieved now by diode array side-pumping of neodimium rods. But the efficiency of this type of pumping is somewhat smaller because of the nonideal overlapping of the inversion profile and the desirable lasing mode (TEM_{00}) [1]. This drawback could be avoided at moderate powers by the use of end-pumping by diode-arrays or several diodes that results in a highly efficient fundamental-mode operation [2]. Nevertheless this kind of end-pumping leads to significant heating of the active element [3], because the pumped region of the crystal should be sufficiently small to select the TEM_{00} mode. These are the reasons which limit the output power in the standard end-pumping scheme, although the use of moving slabs and rotating disks could overcome some of the above difficulties [3]. The alternative approach is to refuse from the gaussian beams paradigm and to select spatially periodic modes using the phenomenon of self-imaging [4].

This approach has proven to be efficient for the phase locking of CO_2 laser sets [5] and antiguided diode-arrays [6]. In this way the simplest scalable solid-state laser resonator could be formed by a thin nonlinear amplifying slice Nd:YAG, Ho:YAG, etc.) end-pumped by diode arrays through the rear surface. In this case a transversely periodic distribution of inversion could be induced inside the amplifying slice (see fig. 2 from ref. [4] and fig. 1 from ref. [7]). When the resonator length is adjusted to be a multiple of $p^2/2\lambda$, where p is the period of inversion, and λ is the lasing wavelength, the Talbot self-imaging leads to the formation of spatially periodic modes, which could be approximated as an equidistinct array of phase-locked quasi-gaussian beams (the first, to our knowledge, discussion of diffractive coupling of lasers is in ref. [8]). Note, that recently after an experimental realization of the akin geometry of pumping had been reported [7]. Under these conditions and when the number of elements is infinite, the simple point-map model of the resonator taking into account inhomogeneous gain profile, gain saturation and self-imaging permits to plot the distribution of the intensity in the near field [4]. Of course this simple picture is somewhat complicated in real resonators which have finite aperture, hence a finite number of elements of amplifying array, and intracavity phase distortions such as thermal lenses and the roughness of mirrors and of the active element

[9–11]. Our job here is to study the just mentioned effects in a numerical model which will enable us to display the transverse modes formation along with the behaviour of the near field wavefront and far-field intensity for the different kinds of intracavity inversion distribution: from a low Fresnel number resonator pumped by a single diode to a high Fresnel number resonator pumped by a diode-array.

2. Preliminary estimates

As previously studied Talbot cavities for CO_2 laser sets [5] and antiguided (leaky-mode) AlGaAs diode arrays [6], this solid-state resonator can be considered as an equidistant array of optically interconnected lasers. It is probable that the Fresnel number $\tilde{N}_f$ of each local solid-state laser placed in a Talbot cavity is always less than unity. In fact, the local Fresnel number is defined as usually as $\tilde{N}_f = d^2/L_r\lambda$, where d is the effective size of the inversion pixel (produced by some diode from the array). Hence, if the resonator length L_r is equal to half the Talbot one, i.e. $L_r = p^2/\lambda$, the local Fresnel number is equal to d^2/p^2. Taking into account that the period of the inversion is greater than the size of the pixel it is easily to obtain that $\tilde{N}_f < 1$. Hence, each individual laser should emit a single transverse mode beam [12].

The Fresnel number for the array as a whole, N_f, should contain another transverse size $D = (N_p - 1)d$, where N_p is the number of elements of the amplifying array (number of diodes in the pumping array). Let all local lasers be synchronized over the whole aperture. So the global Fresnel number is

$$N_f = D^2/L_r\lambda = (N_p - 1)^2 p^2/\lambda(p^2/\lambda) = (N_p - 1)^2 .$$

Similarly if one chooses the resonator length to be equal to one quarter of the Talbot length (in order to provide the selection of an antiphase periodic mode), the global Fresnel number of $N_f = 2(N_p - 1)^2$. Thus we see that a Talbot cavity is essentially a wide aperture one (because a very large number of Fresnel zones takes part in the forming of the eigenmode) and paraxial at the same time (because each amplifying pixel acts as a low Fresnel number laser). The transverse distribution of the intensity on the rear mirror for a large N_p (strictly speaking, when $N_p = \infty$), is given by the exact solution of ref. [4] (eq. (9)), which was obtained by solving the rate equations for a diffractionless, plane wave counter-amplification of the two waves within the thin active slice (as in Rigrod's solution, ref. [13]). It was assumed also, that diffraction outside the active slice only self-images the transversely periodic wave after each resonator roundtrip onto the active slice:

$$I(x, y) = [\ln R_0 + 2\sigma L N(x, y)]/[(1 - R_0)2\sigma T_1] , \quad (1)$$

where σ is the stimulated transition cross-section, T_1 the inversion lifetime, L the width of the active slice. It is easily seen from eq. (1) that the intensity profile coincides with the profile of the inversion. The latter is assumed to have the form of an infinite periodic array of gaussian gain pixels; so that surviving mode could be approximated by an infinite periodic array of phase-locked gaussian beams.

3. Numerical modelling

The numerical modelling was performed by the conventional Fox–Lee method [13] taking into account the saturable amplification inside the active slice and free-space propagation of the amplified field to the output mirror and back again during each cavity roundtrip:

$$E_{n+1}(x, y) = (ik/2\pi L_r) \exp(ikL_r) \times \int_{-\infty}^{+\infty}\int \exp\{-ik[(x - x')^2 + (y - y')^2]/2L_r\} \times g[N(x', y'), E_n(x', y')] \times D(x', y')\, E_n(x', y')\, dx'\, dy' , \quad (2)$$

where $E_n(x, y)$ is the backward intracavity field before entering the amplifying slice, $k = 2\pi/\lambda$, $D(x, y)$ is the complex aperture function (see ref. [10]), g is the nonlinear saturable, transversely periodic gain (eq. (9)) of ref. [4]. The Fresnel–Kirchoff integral was estimated by commonly available FFT routines. The initial wave $E_0(x, y)$ was taken in all runs in the form of a multimode random process (exactly the same as in ref. [10]), the mean intensity being 100 times below saturation. For each given configuration of the resonator these Monte-Carlo runs were re-

peated several times with different realizations of the random phases ψ_m in order to ensure the independence of the surviving eigenmode from the random initial intracavity field. After the first iterates the periodic inversion profile inside the Talbot cavity provided a severe cancellation of the high spatial harmonics (due to $\tilde{N}_f < 1$) and only the smooth fields were obtained.

Firstly it was tested that an inversion distribution in the form of a single gaussian pixel provides the selection of the usual TEM_{00} eigenmode both in one and two transverse dimensions (as expected). The gradual increasing of the number of pixels N_p from 3 to 64 have lead to the gradual transition from TEM_{00} gaussian picture to the almost purely periodic eigenmode as shown in fig. 1. This transition is explained by estimates of the global Fresnel number N_f from a previous section. For $N_p = 3$ the N_f is equal to 4 and TEM_{00} selection is still good (fig. 1a). For $N_p = 5$ the N_f is equal to 16 and the surviving mode is intermediate between TEM_{00} and periodic (fig. 1b). For $N_p = 64$ the diffraction at the edges of the amplifying array is relatively small and the surviving mode is highly correlated with exact solution (1) for an ideal Talbot cavity. Correlation K has been defined as usually as a normalized scalar product (see ref. [10]). Yet, the approximation of the near-field intensity in the form of the transversely periodic array will be still good for $N_p = 16$, when the Fresnel number $N_f = 225$.

The two-dimensional numerical modelling shown as an initial speckle pattern whose intensity distribution consisted formely of a set of irregularly located humps and wavefront dislocations (vortexes) located at zeros of intensity, was gradually transformed into a spatially periodic array of phase locked gaussian beams. In fig. 2 the surviving transverse structure is represented for a 5×5 amplifying array, the intensity distributed being close to the product of two 1D distributions (x and y dependent) of fig. 1b. Note that inside the amplifying array the intensity of the surviving mode had no zeros, so the wavefront had no dislocations. Intracavity random phase distortions of 0.2λ were introduced, the wavefront has been close to flat but it was somewhat tilted and correspondingly the far field was somewhat deflected. The far field fwhm was 10% greater than the diffraction limit for $N_p = 5$ and about 30 percent of

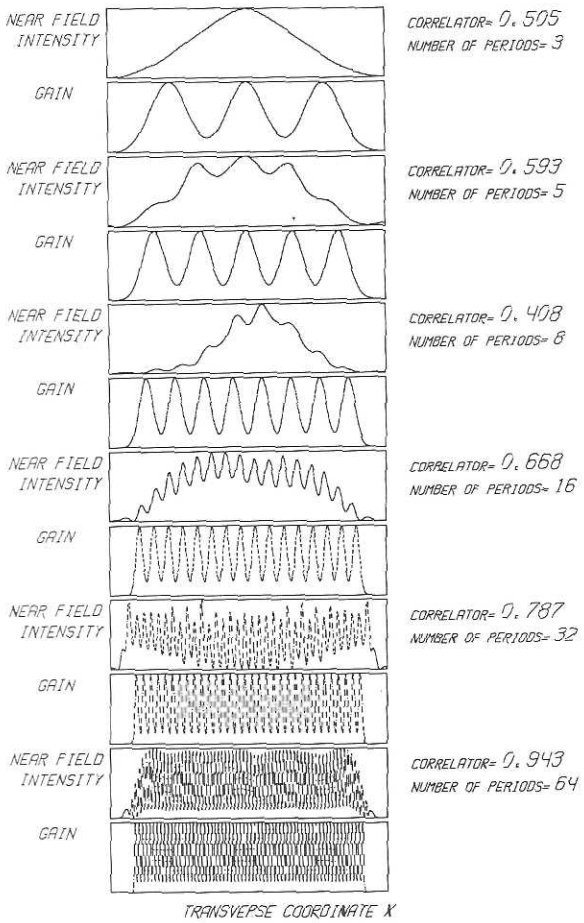

Fig. 1. Transverse distribution of the field on the rear mirror for different numbers of elements in an amplifying array (the distribution on the output mirror is shifted on the half period, because L_r is equal to half the Talbot one). Each pair of windows shows the distribution of intensity (upper window) and corresponding gain (lower window). The number of elements of the amplifying array is varied from 3 (a) to 64 (e). For each pair of figures there are imprinted the corresponding values of the correlator between the calculated intensity distribution and exact solution (eq. (1)), which is proportional to the gain.

the near field power has been diffused outside the far field central lobe.

The finite thickness amplifying slice has been modelled by the split-end FFT method [14] in one transverse dimension for an 8-element array. The number of sections within the active slice was 10. The relative width of the active slice L/L_r has been varied from 0.05 to 0.3. In the case of zero roughness

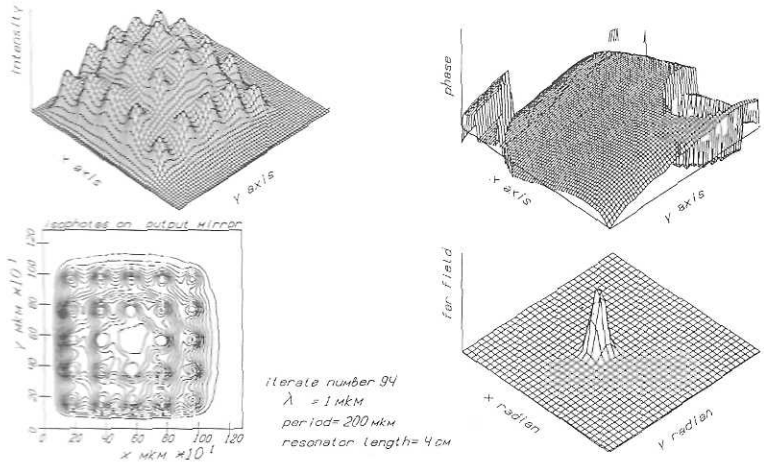

Fig. 2. Two-dimensional intensity (a), phase (b) and far field (c) distributions on the output mirror for a 5×5 amplifying array.

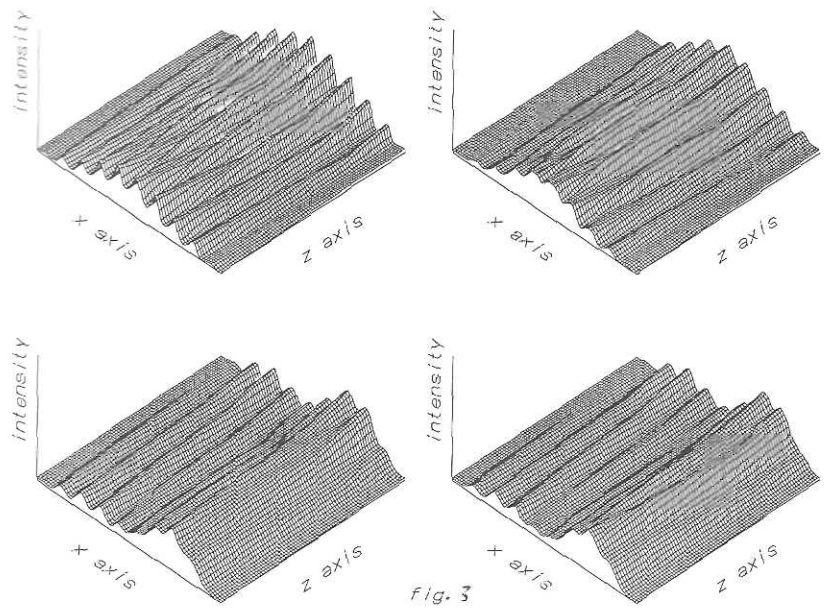

Fig. 3. The distribution of the intensity inside the 8 element diode-pumped solid-state laser resonator (one transverse dimension x is taken into account, z is the optical axis of the resonator) for different values of the thickness of the amplifying slice: (a) $L=0.05\,L_r$, (b) $L=0.1\,L_r$, (c) $L=0.15\,L_r$, (d) $L=0.3\,L_r$.

the spatial layout of the intracavity field (fig. 3a) was the same for all values of L/L_r and well correlated with the thin slice picture, although the interference between adjacent quasi-gaussian beams occurred within the active slice. The mean roughness being equal to 0.1λ has led to a destructive interference within the active slice and in-phase lasing was gradually changed to antiphase at L/L_r (see fig. 3).

4. Conclusions

In this paper we have used the well known simple

numerical model [8,13,14], using the representation of the active medium as a thin nonlinear slice. Within the framework of this model was have observed a continuous transition from the infinite aperture ideal Talbot laser, being pumped by an infinite diode array, to the finite aperture laser: the correlation of the intracavity field with inversion distribution, which is very close to unity for the single diode-pumping, is again increased up to 0.94 along with the increase of the number of amplifying pixels. Two-dimensional modelling of 5×5 solid-state laser arrays showed that the transverse structure is qualitatively the same as in the absence of phase distortions, but some part of the power is diffused outside the central lobe. In the presence of intracavity phase distortions the spatial overlapping within the thick active slice and subsequent destructive interference of quasi-gaussian beams emitted by adjacent amplifying pixels is undesirable because it disturbs the spatial periodicity and the diffraction-limited in-phase lasing. Although Kubota [7] has experimentally succeeded in selection of the TEM_{11} Gauss–Hermite mode, a further scaling of the $N\times N$ solid-state laser arrays could require the selection of Talbot modes, which are somewhat better suited for scaling, than the Gauss–Hermite ones, because the latter require to form a nonequidistant grating of inversion.

References

[1] P. Hanson and D. Haddock, Appl. Optics 27 (1988) 80.
[2] T.J. Fan, A. Sanchez and W.E. DeFeo, Optics Lett. 14 (1989) 1312.
[3] R.L. Byer and S. Basu, Appl. Optics 29 (1990) 1765.
[4] A.Yu. Okulov, J. Opt. Soc. Am. B 7 (1990) 1045.
[5] V.V. Antyuhov, A.F. Glova, O.P. Katchurin, F.V. Lebedev, V.V. Likhansky, A.P. Napartovich and V.D. Pysmennyi, JETP Lett. 44 (1986) 78..
[6] J.Z. Wilcox, W.W. Simmons, D. Botez, M. Jansen, J.L. Mawst, G. Peterson, T.J. Wilcox and J.J. Yang, Appl. Phys. Lett. 54 (1989) 1848.
[7] M. Oka, H. Masuda, Y. Kaneda and S. Kubota, J. Quantum Electron. QE-28 (1992) 1142.
[8] N.G. Basov, E.M. Belenov and V.S. Letokhov, Sov. J. Tech. Phys. 35 (1965) 1098.
[9] A.A. Golubentsev and V.V. Likhansky, Sov. J. Quantum Electron. 17 (1990) 592.
[10] A.Yu. Okulov, J. Mod. Optics 38 (1991) 1887.
[11] W.J. Cassarly, J.C. Ehlert, M. Finlan, K.M. Flood, R. Waarts, D. Mehuys, D. Nam and D. Welch, Optics Lett. 17 (1992) 607.
[12] L.A. Weinstein, Open resonators and open waveguides (Golem Press, Boulder, Colorado, 1969) Ch. 1.
[13] A.E. Siegman, Lasers (University Science Books, Mill Valley, CA, 1986) Ch. 22.
[14] A.E. Siegman and E.A. Sziklas, Appl. Optics 14 (1974) 1874.